Fluid mixtures in nanotubes

Fluid Mixtures in Nanotubes.

Henri Gouin[1†], Augusto Muracchini[2], and Tommaso Ruggeri[2]
[1]*Aix Marseille Univ, CNRS, IUSTI UMR 7343, 13453 Marseille, France*
[2]*Department of Mathematics, University of Bologna, 40123 Bologna, Italy* *
(Dated: April 24, 2018)

The aim of the paper is the study of fluid mixtures in nanotubes by the methods of continuum mechanics. The model starts from a statistical distribution in mean-field molecular theory and uses a density expansion of Taylor series. We get a continuous expression of the volume free energy with density's spatial-derivatives limited at the second order. The nanotubes can be filled with liquid or vapor according to the chemical characteristics of the walls and of liquid or vapor mixture-bulks. An example of two-fluid mixture constituted of water and ethanol inside carbon nanotubes at 20° C is considered. When diameters are small enough, nanotubes are filled with liquid-mixture whatever are the liquid or vapor mixture-bulks. The carbon wall influences the ratio of the fluid components in favor of ethanol. The fluid-mixture flows across nanotubes can be much more important than classical ones and if the external bulk is vapor, the flow can be several hundred thousand times larger than Poiseuille flow.

PACS Numbers: 61.46.Fg, 61.20.Gy, 68.35.Md, 47.61.-k
Keywords: nanotubes; fluid mixtures; nanotube flows, Fluid-mixture/solid interactions.

I. INTRODUCTION

The technical development of sciences allows us to observe phenomena at length scales of a very few number of nanometers. The observations reveal new behaviors that are often surprising and essentially different from those usually observed at a microscopic or macroscopic scales [1, 2]. Experiments prove that liquid densities change in very narrow pores [3] and the conventional laws of capillarity are disqualified when they are applied to fluids confined inside porous materials [4]. Iijima, the discoverer of carbon nanotubes [5], was fascinated by Krätschmer *et al*'s paper [6] and decided to launch out into a detailed study of nano-materials. Since the late 1900s the literature has become abundant regarding technology and flows inside nanotubes [7]. Nevertheless, simple models proposing qualitative behaviors need to be developed.
In this paper, our aim is to investigate an example of mixture-solid interaction in statics as well as in dynamical conditions by using the methods of continuum mechanics. These continuous methods are experimentally realistic until nanotube diameter sizes of a very small number of nanometers [8]
To propose an analytic expression of densities for mixture-films of nanometric thicknesses near a smooth solid wall, we add an interaction energy at the solid wall to a density-functional which represents the volume free energy of the mixture [9–11]. These two energies are obtained by series expansions using London's potentials for fluid-fluid and fluid-solid interactions [12]. The functional is extended from studies by van der Waals, Cahn and Hilliard and many others [13–16].

We consider a nanotube made up of a cylindrical hollow tube whose diameter is of a few number of nanometers. The length of the nanotube is of microscopic size and the cylinder wall is solid [1]. The nanotube is immersed in an homogeneous liquid or vapor bulk made up with two fluids which fill the interior of the nanotube.
In nanofluidics, the interactions between fluids and solid walls can dominate over the hydrodynamic behaviors. The mixture compressibility near a solid wall is extremely important [3]. In liquid or vapor bulks, we express the chemical potentials of fluid-components with only a first-order development taking account of isothermal sound-velocities of single bulks [2]. The equations of equilibrium and motion of fluid mixtures inside the nanotube take the fluid super-deformations into account [9]. In cylindrical representation, two differential equations are obtained and the profiles of the fluid-mixture densities in the cylinder can be deduced.

The results are applied to carbon nanotubes filled with a mixture constituted of water and ethanol and extend those obtained for simple fluids in [17, 18]. The nanotube diameter ranges from 1 to 100 nanometers. Due to energetic properties, the case of liquid and vapor separated by an interface inside the nanotube is not possible when the nanotube diameter is small enough. The mixture inside nanotubes is liquid and the ratio between water and ethanol significantly changes from the mixture-bulk ratio. Recently, it was shown, by using non-equilibrium molecular dynamics simulations, that liquid flows through a membrane composed of an array of aligned carbon nanotubes are a lot faster than it would be predicted by conventional fluid-flow theory [19]. These high velocities are

* † Author for correspondence: Henri Gouin
henri.gouin@univ-amu.fr; henri.gouin@yahoo.fr,
Other E-mails:
augusto.muracchini@unibo.it, tommaso.ruggeri@unibo.it

possible because of a frictionless surface at the nanotube wall [20]. By calculating the variation of viscosity and slip length as a function of the nanotube diameters, the results can be fully explained in the context of continuum fluid mechanics [21]. In our model, we find that a spectacular effect must appear for tiny carbon nanotubes when the mixture bulk outside the nanotube is constituted of vapor: the mixture flows through the nanotube can be multiplied by a factor of several hundred thousand times what is found for Poiseuille's model.

The paper is organized as follows:
In Section 2, thanks to the mean-field theory with hard-sphere molecules, we present a continuous form of free energy for inhomogeneous mixtures. In Section 3, the equations of equilibrium and boundary conditions at a solid wall are written. In Section 4, we consider the chemical potentials of fluid components near a phase and in Section 5, we study the special case of ethanol and water mixture in carbon nanotubes. Thanks to Hamaker's constants, we can determine the profiles of densities at equilibrium. When the pressure of vapor bulk is not too important with respect to the liquid bulk pressure, the carbon nanotube is filled by liquid mixture. Numerical computations yield the densities profiles of water and ethanol inside the nanotubes. In Section 6, the results are extended in the motion case and, as it is experimentally verified, with a classical viscosity. A conclusion ends the paper.

II. A SECOND-GRADIENT FLUID-MIXTURE ENERGY

In a single fluid where the density is not uniform, the intermolecular forces exert on a given molecule a resultant force accounting for the effects of surface tension [22]. The force derives from a system of pressures and stresses that differs from the classical isotropic pressure, which assumes uniformity of density. The kinetic theory of the gases makes it possible to obtain this system of tension and allows us to study the equilibrium of the fluid by layers of equal density and produces a good modelization of the superficial tension. It has been known for a long time, that the law of statistical distribution of molecules around one of them is almost inaccessible even for a distribution of uniform density [23]. If we take a regularized law of distribution at a distance of a given molecule, then we ignore density fluctuations, but the effect of fluctuations tends to be eliminated by integration. This is why, it seems to us possible to approach the problem of the field of forces without presupposing the problem solved and without knowing the true distribution of the molecules. An important property is that the probability of presence of a molecule at a distance less than the molecular diameter is zero. The potential of intermolecular forces is a rapidly decreasing function of distance. It is enough to know the law of distribution at the effective distance and thus the fluctuations of the law beyond this distance no longer influence the result. The case corresponds to the reality given that the preponderant forces are of the type $1/r^7$. It is then possible to develop in series the distribution gap of the molecules. An energy density is then expressed as a measure per unit volume and allows a description in mechanics of continuous media. Such an energy model allows us to obtain a good variation of density in liquid-vapor interfaces even if they are spherical and of nanometer size [24]. It is even possible to get variation of fluid density in the vicinity of a solid wall. As it is proposed in [12], we can extend the model for inhomogeneous fluid mixtures. Then, it is possible to propose analytic expressions for the interaction potentials in terms of densities of the two species of a mixture and consequently to get a continuum mechanics description of volume energy which is valid at nanometer size of interfaces.

A. Energy per unit volume

In the mean-field theory with hard-sphere molecules and for each constituent of a fluid-mixture, the fluid's molecules are identical. The central forces between molecules of constituent i, $i \in \{1,2\}$ derive from a potential $\varphi_i(r)$ and between molecules of the two constituents from a potential $\varphi_3(r)$, where r is the distance between the centers of the two molecules [25].
In three-dimensional Euclidean medium $\mathcal{D}$, the potential energy W_{o1} resulting from the combined action of all the molecules on the molecule of constituent 1, located at origin O, is assumed to be additive such that

$$W_{o1} = \sum_{N_1} \varphi_1(r) + \sum_{N_2} \varphi_3(r),$$

where N_1 denotes all molecules of constituent 1 (except for the molecule located at origin O) and N_2 of constituent 2, respectively; r denotes the distance of molecules to the molecule of constituent 1 located at O. With similar notations, we get

$$W_{o2} = \sum_{N_2} \varphi_2(r) + \sum_{N_1} \varphi_3(r).$$

The number of molecules of constituent i in volume dv is represented by $n_i(x,y,z)\,dv$, where dv denotes the volume element in $\mathcal{D}$ at point of coordinates x, y, z, and in a continuous representation,

$$W_{o1} = \iiint_{\mathcal{D}} \varphi_1(r)\, n_1\, dv + \iiint_{\mathcal{D}} \varphi_3(r)\, n_2\, dv,$$

with

$$\iiint_{\mathcal{D}} \varphi_1(r)\, n_1\, dv = \int_{\sigma_1}^{\infty} \varphi_1(r) \left[\iint_{S(r)} n_1\, ds \right] dr,$$

and

$$\iiint_{\mathcal{D}} \varphi_3(r)\, n_2\, dv = \int_{\frac{1}{2}(\sigma_l+\sigma_2)}^{\infty} \varphi_3(r) \quad \left[\iint_{S(r)} n_2\, ds \right] dr,$$

where ds is the measure of area, $S(r)$ is the sphere of center O and radius r, and σ_i is the molecular diameter of molecules of

component i, $i \in \{1,2\}$. We assume that $n_i(x,y,z)$, $i \in \{1,2\}$ are analytic functions of coordinates x, y, z, *i.e.*

$$n_i = n_i(0,0,0) + \sum_{\ell=1}^{\infty} \frac{1}{\ell\,!}\left[x\frac{\partial n_i}{\partial x}(0,0,0) + y\frac{\partial n_i}{\partial y}(0,0,0) + z\frac{\partial n_i}{\partial z}(0,0,0)\right]^{(\ell)}.$$

The method will be specially justified in two cases:
(*a*) $\varphi_k(r)$, $k \in \{1,2,3\}$, are constant over a large diameter: then the distribution fluctuations of the following molecules are eliminated, this would be the case for van der Waals forces with a large radius of action.
(*b*) $\varphi_k(r)$, $k \in \{1,2,3\}$, are rapidly decreasing functions of distance: It suffices to know the law of distance distribution of molecules at the effective distance, that is, very close to one of them, and then the fluctuations of the law at a great distance, or even at a distance a little greater, no longer influence the result.
In fact, the second case corresponds to reality since the predominant forces which we will have to count with, are of type $1/r^7$. It is then possible to develop in series the difference of n_i with respect to its value in O and to limit to the second order. All these comments are developed in [15, 22].
We notice that for any integers p, q, r we have the relations

$$\iint_{S(r)} x^{2p+1} y^q z^r ds = 0,$$

and

$$\iint_S x^2 ds = \iint_S y^2 ds = \iint_S z^2 ds = \frac{4\pi r^4}{3}.$$

Then,

$$W_{o1} = \int_{\sigma_1}^{\infty} \varphi_1(r)\left[4\pi r^2 n_{1o} + \frac{2\pi}{3} r^4 \Delta n_{1o}\right] dr + \int_{\frac{1}{2}(\sigma_1+\sigma_2)}^{\infty} \varphi_3(r)\left[4\pi r^2 n_{2o} + \frac{2\pi}{3} r^4 \Delta n_{2o}\right] dr.$$

Here $n_{io} \equiv n_i(0,0,0)$, $\Delta n_{io} \equiv \Delta n_i(0,0,0)$, $i \in \{1,2\}$ and Δ is the Beltrami-Laplace operator. Let us denote

$$2\,m_1^2\,k_1 = \int_{\sigma_1}^{\infty} 4\pi r^2 \varphi_1(r)\,dr,$$
$$2\,m_1^2\,k_1\,b_1^2 = \int_{\sigma_1}^{\infty} \frac{2\pi}{3} r^4 \varphi_1(r)\,dr,$$
$$2\,m_1 m_2\,\kappa_3 = \int_{\frac{1}{2}(\sigma_1+\sigma_2)}^{\infty} 4\pi r^2 \varphi_3(r)\,dr,$$
$$2\,k_3\,m_1 m_2\,b_3^2 = \int_{\frac{1}{2}(\sigma_1+\sigma_2)}^{\infty} \frac{2\pi}{3} r^4 \varphi_3(r)\,dr,$$

where σ_i, $i \in \{1,2\}$, denotes molecular diameters of fluids, b_1 is the fluid's co-volume of component 1 [22] and b_3 is analog to a fluid's co-volume between components 1 and 2. To define different mass densities ρ_i of components i, we must introduce the molecular masses of species denoted m_i; then, $\rho_i = n_i m_i$ and

$$W_{o1} = 2\,m_1^2\,k_1\left[n_{1o} + b_1^2\,\Delta\,n_{1o}\right] + 2\,m_1 m_2\,k_3\left[n_{2o} + b_3^2\,\Delta\,n_{2o}\right],$$

We deduce,

$$W_{o1} = 2\,m_1\,k_1\,\left[\rho_{1o} + b_1^2\,\Delta\rho_{1o}\right] + 2\,m_1\,k_3\left[\rho_{2o} + b_3^2\,\Delta\,\rho_{2o}\right],$$

where $\rho_{io} = n_{io} m_i$, $i \in \{1,2\}$ are the mass densities of components i at O. Similarly, we obtain

$$W_{o2} = 2\,m_2\,k_2\,\left[\rho_{2o} + b_2^2\,\Delta\rho_{2o}\right] + 2\,m_2\,k_3\left[\rho_{1o} + b_3^2\,\Delta\,\rho_{1o}\right].$$

We have to consider that all couples of molecules of the two components are counted twice and the double of the potential energy density per unit volume is

$$2\,(n_{1o}\,W_{o1} + n_{2o}\,W_{o2}) \equiv 2\,(E_{o1} + E_{o2}),$$

with

$$\begin{cases} E_{o1} = n_{1o}\,m_1\,k_1\,\left[\rho_{1o} + b_1^2\,\Delta\rho_{1o}\right] + n_{1o}\,m_1\,k_3\left[\rho_{2o} + b_3^2\,\Delta\,\rho_{2o}\right], \\ E_{o2} = n_{2o}\,m_2\,k_2\,\left[\rho_{2o} + b_2^2\,\Delta\rho_{2o}\right] + n_{2o}\,m_2\,k_3\left[\rho_{1o} + b_3^2\,\Delta\,\rho_{1o}\right]. \end{cases}$$

The corresponding potential energy of the two-fluid mixture becomes

$$W = \iiint_{\mathcal{D}} \Big\{k_1\left[\rho_1^2 + b_1^2\,\rho_1\,\Delta\rho_1\right] + k_2\left[\rho_2^2 + b_2^2\,\rho_2\,\Delta\rho_2\right] + k_3\left[2\rho_1\,\rho_2 + b_3^2\,\rho_1\,\Delta\rho_2 + b_3^2\,\rho_2\,\Delta\rho_1\right]\Big\} dv.$$

Taking account of

$$\rho_i\,\Delta\rho_j = \rho_i\,\mathrm{div}\left(\nabla\,\rho_j\right) = \mathrm{div}\left(\rho_i\,\nabla\,\rho_j\right) - \nabla\,\rho_i\,\nabla\,\rho_j,$$

where ∇ is the gradient operator, terms $\mathrm{div}\left(\rho_i\,\nabla\,\rho_j\right)$, with $i, j \in \{1,2\}$, are integrable on the boundary of $\mathcal{D}$, where ρ_1 and ρ_2 are assumed uniform and yield a zero contribution to W. We get

$$W = \iiint_{\mathcal{D}} \Big\{k_1\,\rho_1^2 + k_2\,\rho_2 + 2\,k_3\,\rho_1\,\rho_2 - k_1\,b_1^2\,(\nabla\rho_1)^2 - k_2\,b_2^2\,(\nabla\rho_2)^2 - 2\,k_3\,b_3^2\,\nabla\rho_1\,\nabla\rho_2\Big\}\,dv. \quad (1)$$

To obtain the volume free energy at given temperature T, we have to take account of the kinetic effects of molecular motions where the first terms $k_1\,\rho_1^2 + k_2\,\rho_2^2 + 2\,k_3\,\rho_1\,\rho_2$ in Eq. (1) correspond to the total internal pressure [22]. Consequently, the volume free energy reads

$$\varepsilon = \varepsilon_0(\rho_1,\rho_2) + \frac{1}{2}\left[\,\lambda_1\,(\nabla\rho_1)^2 + \lambda_2\,(\nabla\rho_2)^2 + 2\lambda_3\,\nabla\rho_1\,\nabla\rho_2\,\right], \quad (2)$$

where $\varepsilon_0(\rho_1,\rho_2)$ is the volume free energy of the homogeneous fluid-mixture when densities are ρ_1, ρ_2 (for the sake of simplicity, we omit to indicate T in ε_0) and

$$\lambda_1 = -2\,k_1\,b_1^2, \quad \lambda_2 = -2\,k_2\,b_2^2, \quad \text{and} \quad \lambda_3 = -2\,k_3\,b_3^2\,. \quad (3)$$

Let us note that coefficients k_1, k_2, k_3 are negative for intermolecular potentials associated with attractive forces and coefficients $\lambda_1, \lambda_2, \lambda_3$ are positive.

B. Energy per unit area of wall boundary

In 1977, John Cahn gave simple illuminating arguments to describe the interaction between solids and liquids [26]. His model is based on a generalized van der Waals theory of fluids treated as attracting hard spheres [15]. It entailed assigning to the solid surface an energy that was a functional of the liquid density *at the surface*; the particular form of this energy is now widely known in the literature and was thoroughly examined as an ad hoc approximation in a review paper by de Gennes [27]. Three hypotheses are implicit in Cahn's picture,
(*i*) for the liquid density to be taken as a smooth function of the distance from the solid surface, the correlation length is assumed to be greater than intermolecular distances,
(*ii*) the forces between solid and liquid are of short range with respect to intermolecular distances,
(*iii*) the fluid is considered in the framework of a mean-field theory. This means, in particular, that the free energy of the fluid is a classical so-called *gradient square functional*.

The model was justified and for fluid mixtures, an extension of Cahn's model was proposed with the same hypotheses in [12]. The surface is a smooth solid, sharp on an atomic scale and is endowed with a surface energy per unit area of wall $\mathcal{S}$ of domain $\mathcal{D}$. The general form of the surface energy per unit area can be written $e = e(\rho_{1s}, \rho_{2s})$, where ρ_{1s} and ρ_{2s} are values of the fluid densities at the wall. We consider the case when the energy per unit area at the boundary is written as

$$e = -\gamma_{11}\rho_{1s} - \gamma_{21}\rho_{2s} + \frac{1}{2}\left(\gamma_{12}\rho_{1s}^2 + \gamma_{22}\rho_{2s}^2 + 2\gamma_{32}\rho_{1s}\rho_{2s}\right), \quad (4)$$

where γ_{11}, γ_{21}, γ_{12}, γ_{22}, and γ_{32} are positive coefficients expressing the wall's quality with respect to the two-fluid components of the mixture. Values of the coefficients have been proposed in [12] for the case of London's potentials and can be calculated with molecular quantities and Hamaker's constants.

C. van der Waals' forces and Hamaker's constants

We have introduced the intermolecular potentials associated with van der Waals' forces in the form $\varphi(r)$. We consider the case of London's forces between fluids and solid wall and we denote

$$\varphi_{11}(r),\ \varphi_{22}(r),\ \varphi_{ss}(r),\ \varphi_{12}(r),\ \varphi_{1s}(r),\ \varphi_{2s}(r),$$

the London potentials of interactions between fluid 1–fluid 1, fluid 2–fluid 2, solid–solid, fluid 1–fluid 2, fluid 1–solid, fluid 2–solid, respectively. With the notations of Sec. II A and denoting σ_s the molecular diameter of the wall molecules, the London potentials verify

$$\begin{aligned}
&\varphi_{ii}(r) = -\frac{c_{ii}}{r^6},\ \text{where } r > \sigma_i \ \text{ and } \varphi_{ii}(r) = \infty \ \text{ when } r \le \sigma_i, \quad (i = \{1, 2\})\\
&\varphi_{ss}(r) = -\frac{c_{ss}}{r^6},\ \text{where } r > \sigma_s \ \text{ and } \varphi_{ss}(r) = \infty \ \text{ when } r \le \sigma_s,\\
&\varphi_{12}(r) = -\frac{c_{12}}{r^6},\ \text{where } r > \delta_{12} = \frac{\sigma_1 + \sigma_2}{2} \ \text{ and } \varphi_{12}(r) = \infty \ \text{ when } r \le \delta_{12},\\
&\varphi_{is}(r) = -\frac{c_{is}}{r^6},\ \text{where } r > \delta_{is} = \frac{\sigma_i + \sigma_s}{2} \ \text{ and } \varphi_{is}(r) = \infty \ \text{ when } r \le \delta_{is}.
\end{aligned}$$

The intermolecular coefficients denoted by c_{11}, c_{22}, c_{ss}, c_{12}, c_{1s}, c_{2s}, are associated with Hamaker's constants A_{ii} and A_{ss} defined as

$$A_{ii} = \pi^2 N^2 c_{ii} \quad \text{and} \quad A_{ss} = \pi^2 N^2 c_{ss}\,, \quad (5)$$

where N is the number of molecules per unit volume [28, 29]. An important property of Hamaker constants is that they can be experimentally determined. The Hamaker constant between the two dissimilar materials can be estimated in term of Hamaker constants of each material. An approximation is proposed in [30],

$$A_{12} = \sqrt{A_{11}A_{22}}, \quad A_{1s} = \sqrt{A_{11}A_{ss}}, \quad A_{2s} = \sqrt{A_{22}A_{ss}}\,.$$

Expressions of coefficients λ_1, λ_2 and λ_3 can be deduced from Eq. (3),

$$\lambda_1 = \frac{2}{3}\frac{\pi c_{11}}{\sigma_1}, \quad \lambda_2 = \frac{2}{3}\frac{\pi c_{22}}{\sigma_2}, \quad \lambda_3 = \frac{4}{3}\frac{\pi c_{12}}{(\sigma_1 + \sigma_2)}.$$

In the model of London's forces, coefficients γ_{11}, γ_{21}, γ_{12}, γ_{22} and γ_{32} can also be obtained by using intermolecular coefficients. They are proposed in [12] for solid wall of small curvature. Nonetheless, the energy behavior (4) being in the same form for all solid surfaces [27], we will consider the same expressions for the intermolecular coefficients,

$$\gamma_{11} = \frac{\pi c_{1s}}{12\,\delta_{1s}^2}\rho_s, \quad \gamma_{21} = \frac{\pi c_{2s}}{12\,\delta_{2s}^2}\rho_s\,,$$

where ρ_s is the mass density of the solid wall, and

$$\begin{aligned}
\gamma_{12} = \frac{\pi c_{11}}{12\,\delta_{1s}^2}\,, \quad \gamma_{22} = \frac{\pi c_{22}}{12\,\delta_{2s}^2}\,,\\
\gamma_{32} = \frac{\pi c_{12}}{24\,\delta_{2s}^2}\left(\frac{1}{\delta_{1s}^2} + \frac{1}{\delta_{2s}^2}\right).
\end{aligned} \quad (6)$$

III. EQUATIONS OF MOTIONS AND BOUNDARY CONDITIONS FOR INHOMOGENEOUS MIXTURES OF SIMPLE FLUIDS

To obtain the equilibrium equations of mixtures, it is easy to use a variational method. The energy per unit volume is expressed by Eq. (2) and the associated energy of domain $\mathcal{D}$ is

$$E_{\mathcal{D}} = \iiint_{\mathcal{D}} \varepsilon \, dv.$$

The energy per unit area of the wall is expressed by Eq. (4) and the associated energy of surface $\mathcal{S}$ is

$$E_{\mathcal{S}} = \iint_{\mathcal{S}} e \, ds.$$

The potential of the system *fluid mixture–solid wall* is

$$E = \iiint_{\mathcal{D}} \varepsilon \, dv + \iint_{\mathcal{S}} e \, ds.$$

The total masses of components of an isolated and fixed domain $\mathcal{D}$ are

$$M_i = \int_{\mathcal{D}} \rho_i \, dv \quad \text{with} \quad i \in (1,2).$$

When we neglect external forces, as gravity force, the equilibrium of the system is reached when the total energy is minimal and we get the variational equation

$$\delta E - \mu_{01} \, \delta M_1 - \mu_{02} \, \delta M_2 = 0, \tag{7}$$

where μ_{01} and μ_{02} are two constant Lagrange multipliers which have the physical dimension of chemical potentials. Domain $\mathcal{D}$ is the physical domain occupied by the mixture and used to represent the possible states of a mechanical system of particles in thermodynamic equilibrium with a reservoir at given temperature T (we naturally take account of temperature T through term $\varepsilon_0(\rho_1,\rho_2)$ included in ε). To identify the equilibrium state, the Gibbs free energy is minimized. Equation (7) must be valid for all variations $\delta\rho_1$ and $\delta\rho_2$ and consequently,

$$\begin{aligned}&\iiint_{\mathcal{D}} \left(\frac{\partial \varepsilon(\rho_1,\rho_2)}{\partial \rho_1} \delta\rho_1 + \frac{\partial \varepsilon(\rho_1,\rho_2)}{\partial \rho_2} \delta\rho_2 - \mu_{01}\delta\rho_1 - \mu_{02}\delta\rho_2 \right) dv \\ &+ \iint_{\mathcal{S}} \left(\frac{\partial e(\rho_1,\rho_2)}{\partial \rho_1} \, \delta\rho_1 + \frac{\partial e(\rho_1,\rho_2)}{\partial \rho_2} \, \delta\rho_2 \right) ds = 0.\end{aligned} \tag{8}$$

We define

$$\begin{cases} \boldsymbol{\phi}_1 = \lambda_1 \, \nabla\rho_1 + \lambda_3 \, \nabla\rho_2, \\ \\ \boldsymbol{\phi}_2 = \lambda_3 \, \nabla\rho_1 + \lambda_2 \, \nabla\rho_2, \end{cases}$$

and

$$\mu_1(\rho_1,\rho_2) = \frac{\partial \varepsilon(\rho_1,\rho_2)}{\partial \rho_1} \equiv \frac{\partial \varepsilon_0(\rho_1,\rho_2)}{\partial \rho_1},$$

$$\mu_2(\rho_1,\rho_2) = \frac{\partial \varepsilon(\rho_1,\rho_2)}{\partial \rho_2} \equiv \frac{\partial \varepsilon_0(\rho_1,\rho_2)}{\partial \rho_2},$$

which correspond to the chemical potential of the two fluid components at temperature T. Then, Eq. (8) writes

$$\begin{aligned}&\iiint_{\mathcal{D}} \Big[\left(\mu_1(\rho_1,\rho_2) - \mu_{01}\right) \delta\rho_1 + \boldsymbol{\phi}_1 \cdot \delta\nabla\rho_1 \\ &\quad + \left(\mu_2(\rho_1,\rho_2) - \mu_{02}\right) \delta\rho_2 + \boldsymbol{\phi}_2 \cdot \delta\nabla\rho_2 \Big] dv \\ &+ \iint_{\mathcal{S}} \left(\frac{\partial \, e(\rho_1,\rho_2)}{\partial \rho_1} \, \delta\rho_1 + \frac{\partial e(\rho_1,\rho_2)}{\partial \rho_2} \, \delta\rho_2 \right) ds = 0.\end{aligned}$$

Due to

$$\boldsymbol{\phi}_i \, \nabla\delta\rho_i = \operatorname{div}\left(\boldsymbol{\phi}_i \, \delta\rho_i\right) - \left(\operatorname{div}\boldsymbol{\phi}_i\right) \delta\rho_i \text{ and } \nabla\delta\rho_i = \delta\nabla\rho_i \,,$$

and using the divergence theorem, we get

$$\begin{aligned}&\sum_{i=1}^{2} \iiint_{\mathcal{D}} \left(\mu_i(\rho_1,\rho_2) - \mu_{0i} - \operatorname{div} \boldsymbol{\phi}_i\right) \delta\rho_i \, dv \\ &+ \iint_{\mathcal{S}} \left(\frac{\partial e(\rho_1,\rho_2)}{\partial \rho_i} + \boldsymbol{n} \cdot \boldsymbol{\phi}_i \right) \delta\rho_i \, ds = 0,\end{aligned}$$

where $\boldsymbol{n}$ is the external normal to $\mathcal{S}$. First, we obtain the equations of equilibrium

$$\begin{cases} \operatorname{div} \boldsymbol{\phi}_1 \; = \; \mu_1(\rho_1,\rho_2) - \mu_{01}, \\ \\ \operatorname{div} \boldsymbol{\phi}_2 \; = \; \mu_2(\rho_1,\rho_2) - \mu_{02}, \end{cases}$$

which gives

$$\begin{cases} \lambda_1 \Delta\rho_1 + \lambda_3 \Delta\rho_2 \; = \; \mu_1(\rho_1,\rho_2) - \mu_{01}, \\ \\ \lambda_3 \Delta\rho_1 + \lambda_2 \Delta\rho_2 \; = \; \mu_2(\rho_1,\rho_2) - \mu_{02}, \end{cases} \tag{9}$$

and second, the boundary conditions at surface $\mathcal{S}$,

$$\frac{\partial e(\rho_1,\rho_2)}{\partial \rho_1} + \boldsymbol{n} \cdot \boldsymbol{\phi}_1 = 0 \quad \text{and} \quad \frac{\partial e(\rho_1,\rho_2)}{\partial \rho_2} + \boldsymbol{n} \cdot \boldsymbol{\phi}_2 = 0.$$

The previous results – expressed at equilibrium – can be extended to mixture motions by the addition of inertial forces. When we neglect the external forces, as gravity force, the two-liquid mixture motions verify equations extended from the equilibrium case and presented in [31]. They are in the form

$$\begin{cases} \boldsymbol{a}_1 + \nabla[\, \mu_1(\rho_1) - \lambda_1 \, \Delta\rho_1 \; - \lambda_3 \, \Delta\rho_2 \,] = \nu_1 \, \Delta\boldsymbol{v}_1, \\ \\ \boldsymbol{a}_2 + \nabla[\, \mu_2(\rho_2) - \lambda_3 \, \Delta\rho_1 \; - \lambda_2 \, \Delta\rho_2 \,] = \nu_2 \, \Delta\boldsymbol{v}_2, \end{cases} \tag{10}$$

where $\boldsymbol{a}_i,\ \boldsymbol{v}_i,\ \nu_i,\ i \in \{1,2\}$ denote the accelerations, velocities and kinematic coefficients of viscosity of the two-fluid components, respectively. What is unexpected at first, the kinematic coefficients of viscosity are the same as for bulks [8]. The boundary conditions at surface $\mathcal{S}$ are unchanged.

Let us note that chemical potentials naturally introduce isobaric ensembles.

IV. THE CHEMICAL POTENTIALS IN FLUID-COMPONENT BULKS

The two-fluid mixture is constituted of simple compressible fluids. Consequently, pressure and chemical potential are the sum of the pressures and chemical potentials of fluid-components.
In the fluid component bulks corresponding to the plane liquid-vapor interface at temperature T, each chemical potential is denoted by μ_{i0}, $i \in \{1,2\}$. Due to the pressure equation $p_i = p_i(\rho_i, T)$ of fluid-component i, it is possible to express μ_{i0} as a function of ρ_i.
At given temperature T, the associated volume free energy of fluid component i, denoted g_{i0}, verifies $g'_{i0}(\rho_i) = \mu_{i0}(\rho_i)$. Potentials μ_{i0} and g_{i0} are defined except an additive constant and therefore we can choose the conditions

$$\mu_{i0}(\rho_{i\ell}) = \mu_{i0}(\rho_{iv}) = 0 \quad \text{and} \quad g_{i0}(\rho_{i\ell}) = g_{i0}(\rho_{iv}) = 0,$$

where $\rho_{i\ell}$ and ρ_{iv} are the densities in liquid and vapor of the bulks corresponding to the plane liquid-vapor interface of fluid-component i. The expressions of thermodynamical potentials μ_{i0} and g_{i0} can be expanded to the first order near liquid and vapor bulks, respectively

$$\mu_{i0}(\rho_i) = \frac{C_{i\ell}^2}{\rho_{i\ell}}(\rho_i - \rho_{i\ell}) \quad \text{and} \quad \mu_{i0}(\rho_i) = \frac{C_{iv}^2}{\rho_{iv}}(\rho_i - \rho_{iv}),$$

$$g_{i0}(\rho_i) = \frac{C_{i\ell}^2}{2\rho_{i\ell}}(\rho_i - \rho_{i\ell})^2 \quad \text{and} \quad g_{i0}(\rho_i) = \frac{C_{iv}^2}{2\rho_{iv}}(\rho_i - \rho_{iv})^2,$$

where $C_{i\ell}$ and C_{iv} are the isothermal sound-velocities in liquid and vapor bulks of component i [2]. It is possible to obtain the connection between the liquid bulk of density $\rho_{i\ell b}$ and the vapor bulk of density ρ_{ivb} corresponding to non-planar interfaces (as for spherical bubbles and droplets [24]); they are called the mother-bulk densities [32]. These equilibria do not obey the Maxwell rule, but the values of the chemical potential in the two mother bulks must be equal

$$\mu_{i0}(\rho_{i\ell b}) = \mu_{i0}(\rho_{ivb}),$$

and determine the connection between $\rho_{i\ell b}$ and ρ_{ivb}.
Consequently, we define $\mu_{i\ell b}(\rho_i)$ and $\mu_{ivb}(\rho_i)$ as

$$\mu_{i\ell b}(\rho_i) = \mu_{i_0}(\rho_i) - \mu_{i_0}(\rho_{i\ell b}) \equiv \mu_{i_0}(\rho_i) - \mu_{i_0}(\rho_{ivb}) = \mu_{ivb}(\rho_i).$$

An expansion to the first order near the liquid bulk of density $\rho_{i\ell b}$ and the vapor bulk of density ρ_{ivb} yields

$$\mu_{i\ell b}(\rho_i) = \frac{C_{i\ell}^2}{\rho_{i\ell b}}(\rho_i - \rho_{i\ell b}) \quad \text{and} \quad \mu_{ivb}(\rho_i) = \frac{C_{iv}^2}{\rho_{ivb}}(\rho_i - \rho_{ivb}) \tag{11}$$

To the chemical potential $\mu_{i\ell b}(\rho_i) \equiv \mu_{ivb}(\rho_i)$, we can associate the volume free energies $g_{i\ell b}(\rho_i)$ and $g_{ivb}(\rho_i)$ which are null for $\rho_{i\ell b}$ and ρ_{ivb}, respectively,

$$g_{i\ell b}(\rho_i) = g_{i0}(\rho_i) - g_{i0}(\rho_{i\ell b}) - \mu_{i0}(\rho_{i\ell b})(\rho_i - \rho_{i\ell b}), \tag{12}$$
$$g_{ivb}(\rho_i) = g_{i0}(\rho_i) - g_{i0}(\rho_{ivb}) - \mu_{i0}(\rho_{ivb})(\rho_i - \rho_{ivb}). \tag{13}$$

Free energies $g_{i\ell b}(\rho_i)$ and $g_{ivb}(\rho_i)$ are null for the liquid bulk of density $\rho_{i\ell b}$ and the vapor bulk of density ρ_{ivb} of fluid component i, respectively, and contrary to the chemical potentials, they differ by a constant. Moreover, near the liquid and vapor mother-bulks, the volume free energies can be expanded as

$$g_{i\ell b}(\rho_i) = \frac{C_{i\ell}^2}{2\rho_{i\ell b}}(\rho_i - \rho_{i\ell b})^2 \quad \text{and} \quad g_{ivb}(\rho_i) = \frac{C_{iv}^2}{2\rho_{ivb}}(\rho_i - \rho_{ivb})^2.$$

To compare the case of a nanotube filled with liquid-mixture and the case of a nanotube filled with vapor-mixture, we chose as *reference volume free energy* of component i the volume free energy $g_{i\ell b}(\rho_i)$. Due to $\mu_{i0}(\rho_{i\ell b}) = \mu_{i0}(\rho_{ivb})$, the difference of Eq. (12) and Eq. (13) yields

$$g_{i\ell b}(\rho_i) - g_{ivb}(\rho_i) = g_{i0}(\rho_{ivb}) - g_{i0}(\rho_{i\ell b}) - \mu_{i0}(\rho_{i\ell b})(\rho_{ivb} - \rho_{i\ell b}).$$

But, Eq. (12) yields

$$g_{i\ell b}(\rho_{i\ell b}) = 0,$$
$$g_{i\ell b}(\rho_{ivb}) = g_{i0}(\rho_{ivb}) - g_{i0}(\rho_{i\ell b}) - \mu_{i0}(\rho_{i\ell b})(\rho_{ivb} - \rho_{i\ell b}),$$

and consequently,

$$g_{i\ell b}(\rho_i) = g_{ivb}(\rho_i) + g_{i\ell b}(\rho_{ivb}). \tag{14}$$

From Eq. (14), the term $g_{i\ell b}(\rho_{ivb})$ represents the difference between the volume free energies (12) and (13).

V. WATER-ETHANOL MIXTURE IN CARBON NANOTUBES

We denote by $\mathcal{M}$, $\mathcal{L}$ and $\mathcal{T}$ the mass, length and time dimensions, respectively. The dimensions of other physical quantities are,
molecular coefficients: $\mathcal{M}\mathcal{L}^8\mathcal{T}^{-2}$,
masses per unit of volume: $\mathcal{M}\mathcal{L}^{-3}$,
isothermal sound-velocities: $\mathcal{M}\mathcal{T}^{-1}$.
The values of physical quantities are expressed for water and ethanol at 20° Celsius. These values correspond to molecular coefficients, molecular diameters, molecular masses, mass densities, and isothermal sound-velocities of fluid components for liquids and vapors. They are obtained from the books of Israelaschvili [29], the *Handbook of Chemistry and Physics* [33], and the *Microfluidics and Nanophysics Handbook* [30], and are indicated in Table I. Carbon values are referred to nanotubes from Matsumoto *et al*'s paper [34]. Molecular coefficients are deduced from the Hamaker constants thanks to relations (5). The values of Table I together with Eqs. (5) to (6) allow us to obtain the values of $\lambda_1, \lambda_2, \lambda_3, \gamma_{11}, \gamma_{21}, \gamma_{12}, \gamma_{22}, \gamma_{32}$ and those given in Table II.

Physical constants	Intermolecular coefficient	molecular diameter	molecular mass	Bulk density	Isothermal sound velocity
Liquid-water	1.4×10^{-77}	2.8×10^{-10}	2.99×10^{-26}	998	1.478×10^{3}
Vapor-water	1.4×10^{-77}	2.8×10^{-10}	2.99×10^{-26}	9.7×10^{-3}	3.70×10^{2}
Liquid-ethanol	3.71×10^{-77}	4.69×10^{-10}	7.64×10^{-26}	789	1.162×10^{3}
Vapor-ethanol	3.71×10^{-77}	4.69×10^{-10}	7.64×10^{-26}	1.09×10^{-1}	2.30×10^{2}
Nanotube-carbon	0.1014×10^{-77}	1.30×10^{-10}	1.99×10^{-26}	2000	− − −

TABLE I. The physical values associated with water, ethanol and carbon are expressed in *M.K.S. units* (meter, kilogram, second). In the unit system, we notice the very small values of intermolecular coefficients, molecular diameters and molecular masses.

A. Liquid-mixture at equilibrium in carbon nanotubes

In this section, we compare – at equilibrium – the total free energy of a carbon nanotube filled with a mixture of water and ethanol in liquid, vapor and liquid-vapor conditions. The reference volume free energy is $g_{i\ell b}(\rho_i)$. Including the wall-energy, the total free energy per unit of length of the nanotube can be approximated by considering densities ρ_1 (for water) and ρ_2 (for ethanol) of the two components closely equal to $\rho_{1\ell b}$ and $\rho_{2\ell b}$ or ρ_{1vb} and ρ_{2vb} for the liquid and the vapor phases, respectively.

First, we compare the case of a nanotube filled with liquid mixture and a nanotube filled with vapor mixture.

(i) In the case of a nanotube filled of liquid-mixture, total free energy E_1 per unit of length is,

$$\begin{aligned} E_1 \approx{}& \Pi(\rho_{\ell b})\,\pi R^2 \left[g_{1\ell b}(\rho_{1\ell b}) + g_{2\ell b}(\rho_{2\ell b})\right] \\ &+ 2\,\pi R\Big[-\gamma_{11}\,\rho_{1\ell b} - \gamma_{21}\,\rho_{2\ell b} \\ &+ \frac{1}{2}\left(\gamma_{12}\,\rho_{1\ell b}^2 + \gamma_{22}\,\rho_{2\ell b}^2 + 2\gamma_{32}\,\rho_{1\ell b}\,\rho_{2\ell b}\right)\Big], \end{aligned}$$

where $g_{1\ell b}(\rho_{1\ell b}) = 0$ and $g_{2\ell b}(\rho_{2\ell b}) = 0$.

(ii) In the case of a nanotube filled of the vapor-mixture, total free energy E_2 per unit of length is,

$$\begin{aligned} E_2 \approx{}& \pi R^2 \left[g_{1\ell b}(\rho_{1vb}) + g_{2\ell b}(\rho_{2vb})\right] \\ &+ 2\,\pi R\Big[-\gamma_{11}\rho_{1vb} - \gamma_{21}\rho_{2vb} \\ &+ \frac{1}{2}\left(\gamma_{12}\,\rho_{1vb}^2 + \gamma_{22}\,\rho_{2vb}^2 + 2\gamma_{32}\,\rho_{1vb}\,\rho_{2vb}\right)\Big]. \end{aligned}$$

Due to the densities of vapor components,

$$-\gamma_{11}\,\rho_{1vb} - \gamma_{21}\,\rho_{1vb} + \frac{1}{2}\left(\gamma_{12}\,\rho_{1vb}^2 + \gamma_{22}\,\rho_{2vb}^2 + 2\gamma_{32}\,\rho_{1vb}\,\rho_{2vb}\right)$$

is negligible in the estimation of energy with respect to the first two terms. From the expression of partial pressure p_i of component i, $i \in \{1, 2\}$,

$$p_i(\rho_i) = \rho_i\,\mu_{i0}(\rho_i) - g_{i0}(\rho_i) + p_{i0}$$

where p_{i0} is the common value of the pressure in liquid and vapor bulks of plane interface. Equation (12) yields,

$$\begin{aligned} g_{1\ell b}(\rho_{1vb}) + g_{2\ell b}(\rho_{2vb}) = {}& p_1(\rho_{1\ell b}) - p_1(\rho_{1vb}) \\ &+ p_2(\rho_{2\ell b}) - p_2(\rho_{2vb}). \end{aligned}$$

We denote Π_b,

$$\begin{aligned} &\Pi_b = p(\rho_{vb}) - p(\rho_{\ell b}) = \\ &p_1(\rho_{1vb}) - p_1(\rho_{1\ell b}) + p_2(\rho_{2vb}) - p_2(\rho_{2\ell b}), \end{aligned}$$

the difference between pressure $p(\rho_{vb})$ of the vapor mixture and pressure $p(\rho_{\ell b})$ of the liquid mixture. Pressure Π_b is called the mixture *disjoining-pressure* [2, 32]. Consequently,

$$\begin{aligned} E_2 - E_1 \approx{}& 2\,\pi R\Big[\gamma_{11}\,\rho_{1\ell b} + \gamma_{21}\,\rho_{2\ell b} \\ &- \frac{1}{2}\left(\gamma_{12}\,\rho_{1\ell b}^2 + \gamma_{22}\,\rho_{2\ell b}^2 + 2\,\gamma_{32}\,\rho_{1\ell b}\,\rho_{2\ell b}\right)\Big] - \pi R^2\,\Pi_b, \end{aligned}$$

and the vapor mixture is more energetic than the liquid mixture if

$$\begin{aligned} E_2 > E_1 \quad\Longleftrightarrow\quad \Pi_b < \frac{1}{R}\Big[&2\,\gamma_{11}\,\rho_{1\ell b} + 2\,\gamma_{21}\,\rho_{2\ell b} \\ &- \left(\gamma_{12}\,\rho_{1\ell b}^2 + \gamma_{22}\,\rho_{2\ell b}^2 + 2\,\gamma_{32}\,\rho_{1\ell b}\,\rho_{2\ell b}\right)\Big]. \end{aligned} \tag{15}$$

The ratio between volume proportion of water and ethanol is denoted c. In the bulks, the water density is $\rho_{1\ell b} = c\,\rho_{1\ell}$ and the ethanol density is $\rho_{2\ell b} = (1-c)\,\rho_{2\ell}$. By taking account of Table II, we calculated the most unfavorable case for inequality (15) to be verified. One obtain $R_0 = 50$ nm (for a microtube of 0.1 micron diameter) and we get

$$\Pi_b \equiv p(\rho_{vb}) - p(\rho_{\ell b}) \approx 5 \times 10^5 \text{ Pascal} = 5 \text{ atmospheres}.$$

This result comes from the wall quality of carbon nanotubes: terms γ_{11} and γ_{21} take advantage of terms associated with γ_{12}, γ_{22} and γ_{32}, and consequently the energy of vapor mixture is greater than the energy of liquid mixture.

Second, we compare the case of a nanotube filled with liquid mixture and a nanotube filled with a liquid-vapor mixture. When a two-phase mixture is considered, we assume that an interface appears between the liquid and vapor phases. To estimate the value of the liquid-vapor interface, we consider the smallest possible interface area. The smallest area of the liquid-vapor interface separating the two phases corresponds

Physical constants	λ_1	λ_2	λ_3	γ_{11}
Numerical values	1.17×10^{-16}	0.284×10^{-16}	0.49×10^{-16}	77×10^{-6}
Physical constants	γ_{21}	γ_{12}	γ_{22}	γ_{32}
Numerical values	22×10^{-6}	9.7×10^{-8}	1.8×10^{-8}	4.0×10^{-8}

TABLE II. The physical values associated with the contact of water, ethanol and carbon expressed in *M.K.S. units* (meter, kilogram, second).

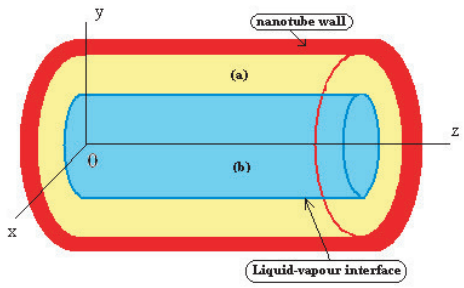

FIG. 1. Two-phase fluid-component in a nanotube: The nanotube is simultaneously filled with two phases liquid and vapor of fluid-components. The two phases (a) and (b) are separated by a cylindrical interface.

to a material surface represented by a cylinder with the same axis as the nanotube axis. The interface has a positive surface energy γ increasing the total fluid energy inside the nanotube (see Fig. 1)

(i) When domain (a) is liquid and domain (b) is vapor, the energy of the wall is approximatively the same as for liquid mixture and the difference of total free energies between liquid mixture and liquid-vapor mixture is approximately

$$E_3 - E_1 \approx \pi\, r_1 \left[\, 2\,\gamma - r_1\, \Pi_b \right],$$

where E_3 is the energy of the two-phase mixture and r_1 is the radius of domain (b).
(ii) When domain (a) is vapor and domain (b) is liquid, the difference of total free energies is approximately

$$\begin{aligned} E_4 - E_1 \approx\; & 2\,\pi\, r_1\, \gamma - \pi \left(R^2 - r_1^2\right) \Pi_b \\ & + 2\,\pi\, R \Big[\, \gamma_{11}\rho_{1vb} + \gamma_{21}\rho_{2vb} \\ & - \frac{1}{2}\left(\gamma_{12}\rho_{1vb}^2 + \gamma_{22}\rho_{2vb}^2 + 2\gamma_{32}\rho_{1vb}\rho_{2vb}\right)\Big], \end{aligned}$$

where E_4 is the energy of the two-phase mixture. The positive interfacial energy associated with γ increases the total energy of the liquid-vapor mixture.
In all cases, when $\gamma > 12.5\times10^{-3}$ N $\times$ m^{-1} (corresponding to a value significantly lower than the surface tension of any water-ethanol mixture at 20° C [33]), and condition (15) is verified, we get

$$E_3 > E_1 \quad \text{and} \quad E_4 > E_1\,.$$

In the following, we consider only carbon nanotubes such that previous conditions are verified. Consequently - at equilibrium - they are filled with liquid mixture of water and ethanol.

Physical units	unit of length	unit of mass	unit of time
Numerical values	2.31×10^{-10} m	1.23×10^{-26} Kg	1.56×10^{-13} s

TABLE III. The new *molecular capillary units*, at temperature T = 20° C, associated with liquid-water are deduced from the Table I and expressed in *M.K.S. units* (meter, kilogram and second).

B. Numerical calculations at equilibrium

We consider cylindrical coordinates (r,θ,z) where z denotes the coordinate of the nanotube axis. Due to the symmetry of revolution and far from nanotube extremities, the densities depend only of z and in the case of liquid mixture, the equations of equilibrium (9) can be written by taking account of Eq. (11),

$$\begin{cases} \lambda_1\left(\dfrac{d^2\rho_1}{dr^2} + \dfrac{1}{r}\dfrac{d\rho_1}{dr}\right) + \lambda_3\left(\dfrac{d^2\rho_2}{dr^2} + \dfrac{1}{r}\dfrac{d\rho_2}{dr}\right) = \dfrac{c_{1\ell}^2}{\rho_{1\ell b}}\,(\rho_1 - \rho_{1\ell b})\,, \\ \lambda_3\left(\dfrac{d^2\rho_1}{dr^2} + \dfrac{1}{r}\dfrac{d\rho_1}{dr}\right) + \lambda_2\left(\dfrac{d^2\rho_2}{dr^2} + \dfrac{1}{r}\dfrac{d\rho_2}{dr}\right) = \dfrac{c_{2\ell}^2}{\rho_{2\ell b}}\,(\rho_2 - \rho_{2\ell b})\,, \end{cases} \tag{16}$$

where ρ_1 and ρ_2 denote the densities associated with water and ethanol, respectively. The symmetry of densities at the z-axis implies,

$$\text{At } r = 0, \quad \frac{d\rho_1}{dr} = 0 \quad \text{and} \quad \frac{d\rho_1}{dr} = 0 \tag{17}$$

and the boundary conditions at the nanotubes wall – where R is the nanotube radius – yield,

$$\text{At } r = R, \quad \begin{cases} \lambda_1\dfrac{d\rho_1}{dr} + \lambda_3\dfrac{d\rho_2}{dr} = \gamma_{11} - \gamma_{12}\,\rho_1 - \gamma_{32}\,\rho_2, \\ \lambda_3\dfrac{d\rho_1}{dr} + \lambda_2\dfrac{d\rho_2}{dr} = \gamma_{21} - \gamma_{32}\,\rho_1 - \gamma_{22}\,\rho_2. \end{cases} \tag{18}$$

For nanotubes, the values obtained in Table II are not expressed in convenient units. To obtain units adapted to the numerical computations, we consider an unit system such that the mass density, the isothermal sound-velocity of liquid-water and λ_1 are equal to 1. Table III indicates the corresponding values of units of length, mass and time. We name these units, *molecular capillary units* at temperature T = 20° C. We notice that the units of length mass and time are of the same order as molecular diameters, masses of molecules and times associated with the mean free paths. In molecular capillary units, the values of $\lambda_1, \lambda_2, \lambda_3, \gamma_{11}, \gamma_{21}, \gamma_{12}, \gamma_{22}$,and γ_{32} are indicated in Table IV.
To easily compare the profiles of densities, we have normalized the diameter with respect to radius R and therefore for all

Physical constants	λ_1	λ_2	λ_3	γ_{11}	γ_{21}	γ_{12}	γ_{22}	γ_{32}
Numerical values	1	0.24	0.42	146	42	3.2×10^{-3}	6×10^{-4}	1.3×10^{-3}

TABLE IV. The physical values associated with water, ethanol and carbon are expressed in *molecular capillarity units*. Moreover, the isothermal sound velocities are $C_{\text{liquid-water}} = 1$ and $C_{\text{liquid-ethanol}} = 0.786$.

figures, the x-axis is drawn between 0 and 1 whatever is the real value of the nanotube diameter.

$c \downarrow 2R \rightarrow$	1 nm	2 nm	3 nm	5 nm	10 nm	20 nm	50 nm	100 nm
$c = 0.3$	2.7%	1.4%	1%	0.6%	0.3%	0.15%	0.1%	0.05%
$c = 0.5$	5%	2.5%	1.7%	1%	0.5%	0.3%	0.2%	0.1%
$c = 0.7$	8.5%	4.4%	3%	1.8%	1%	0.5%	0.37%	0.27%

TABLE V. Percentage of the increase of volume ethanol with respect to volume water for different nanotube diameters and values of ratio c between volume proportion of water and ethanol.

We calculate the profile of densities of the liquid mixture composed of water and ethanol wetting carbon nanotubes. As in Section V A, the ratio between volume proportion of water and ethanol is denoted c, in the bulks, the water density is $\rho_{1\ell b} = c\,\rho_{1\ell}$ and the ethanol density is $\rho_{2\ell b} = (1-c)\,\rho_{2\ell}$. The profiles of densities are given by equilibrium equations (16) and boundary conditions (17)–(18). We calculate three cases of liquid mixtures' composition corresponding in the bulks to $c = 0.3$, 0.5 and 0.7. The density curves depend on nanotube diameters. For each value of c, we calculate the density profiles for water and ethanol when the diameters are 1, 2, 3, 5 , 10, 20, 40 and 100 nanometer. Figures 2, 3 and 4 represent the densities versus r/R for increasing value of R with relative up and down magnifications.
In all cases, we note that the water density decreases near the wall and the profile is monotonic for $c = 0.3$ and $c = 0.5$, and oscillating for $c = 0.7$. For ethanol the density increases near the wall and the profile is oscillating for $c = 0.3$ and $c = 0.5$ and monotonic for $c = 0.7$.
Following ratio c between volume proportion of water and ethanol and the nanotube diameters, volume concentration of ethanol with respect to volume concentration of water increases. The results are indicated on Table V. The effect closely negligible when $c = 0.3$, is noticeable for small nanotubes when $c = 0.7$, and disappears for large nanotubes.

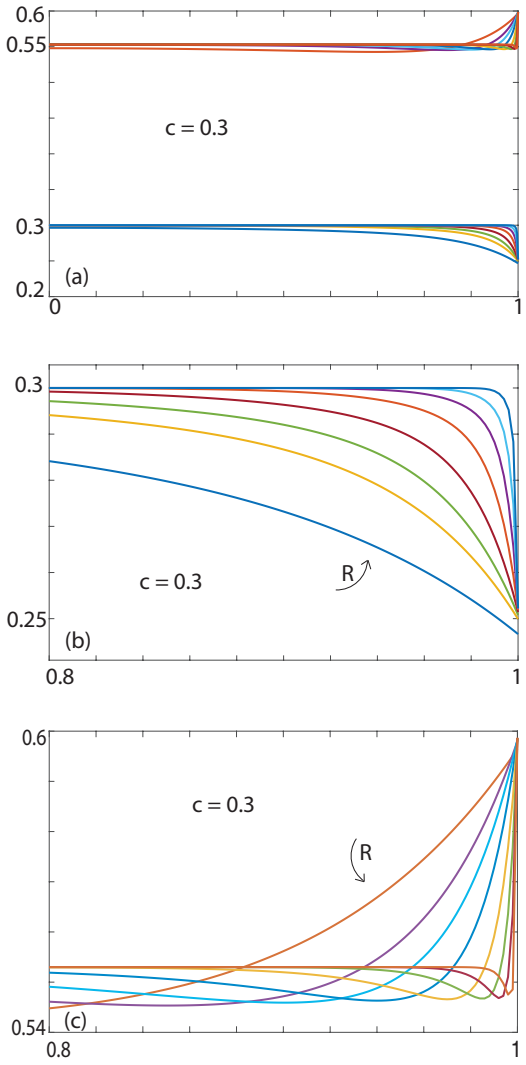

FIG. 2. **Case $c = 0.3$ (corresponding to the volume proportion between water and ethanol in the mixture bulk outside the carbon nanotube).** The different graphs represent the change of the ratio between volume proportion of water and ethanol versus r / R (representing the normalized distance to the carbon wall), when the radius nanotube is successively equal to $R = 0.5$ at 50 nm. *We recall that - to draw all the diameter cases on the same figure - we have normalized the diameter with respect to radius R and therefore, the x-axis is drawn between 0 and 1 for any real value of the nanotube diameter.* The graph (a) shows the density profiles between the nanotube axis and the carbon wall ($r/R \in [0, 1]$). The second graph (b) enlarges the water density near the wall ($r/R \in [0.8, 1]$). The third graph (c) enlarges the ethanol density near the wall ($r/R \in [0.8, 1]$). In the second and third graphs, the curved arrows indicate the different graphs for increasing values of R and for the eight nanotube radius-values corresponding to $2R \in \{1, 2, 3, 5, 10, 20, 50, 100\}$ in nanometers.

VI. VISCOUS MOTIONS IN A NANOTUBE

Fluid flows through structures like carbon nanotubes must be different from flows through microscopic and macroscopic structures since, for the latter flow, the degrees of freedom of fluid molecules can be safely ignored and the flow in such structures can be characterized by viscosity, density and other bulk properties. Furthermore, for large-scale systems, the no-slip boundary condition is often implemented, because the fluid velocity is negligibly small at the fluid/wall boundary. Reducing the length scales introduces new phenomena, when the mutual interaction between walls and fluids must be taken into account [35]. We consider the permanent and laminar motions of viscous capillary liquids in a nanotube. Because the liquid is heterogeneous, the static part of the liquid stress tensor is not scalar and the equations of hydrodynamics are not immediately valid. However, the results obtained for vis-

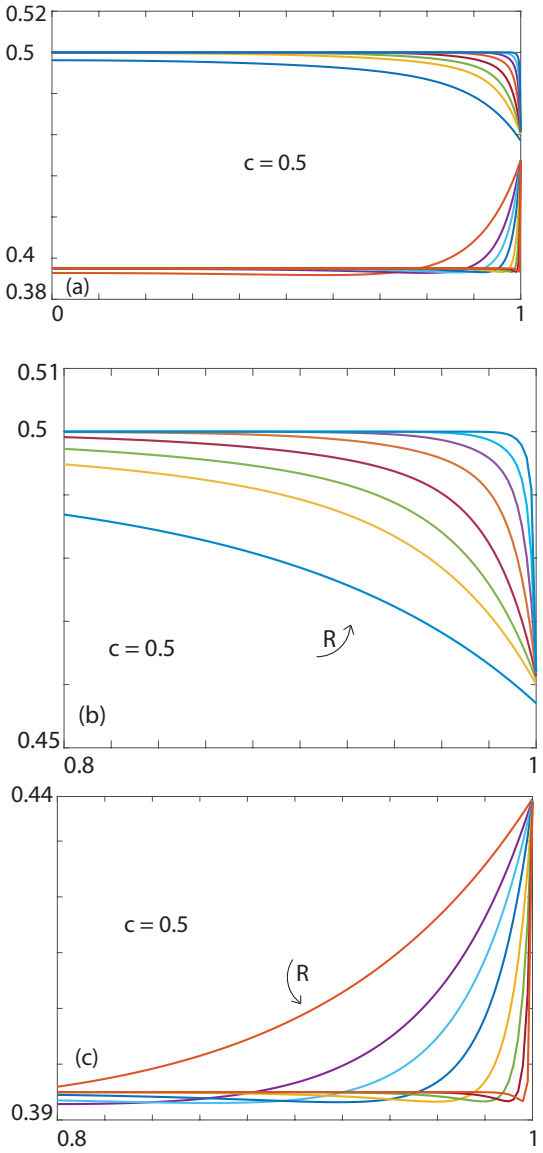

FIG. 3. **Case** $c = 0.5$ **(corresponding to the volume proportion between water and ethanol in the mixture bulk outside the carbon nanotube).** Comments are similar to those for the caption to Fig. 2.

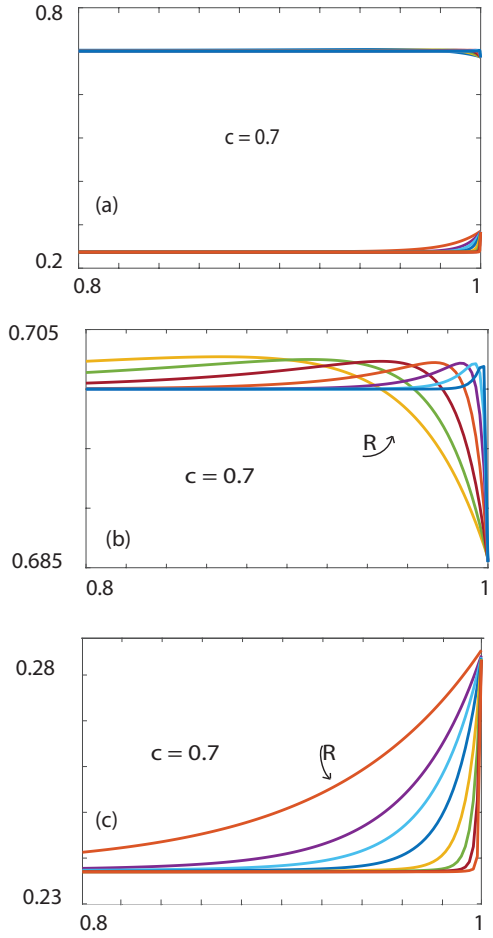

FIG. 4. **Case** $c = 0.7$ **(corresponding to the volume proportion between water and ethanol in the mixture bulk outside the carbon nanotube).** Comments are similar to those for the caption to Fig. 2.

cous flows can be adapted at nanoscales [36]. We denote the velocities by $\boldsymbol{v}_i = (0, 0, w_i)$ where w_i is the velocity of component i of the fluid mixture along the nanotube axis. When we neglect the external forces, as gravity force, the two-liquid mixture motions of the components verify Eqs. (10). Simple fluids slip on a solid wall only at a molecular level and in classical conditions, the kinetic condition at solid wall is the adherence condition ($z = R \Rightarrow w_i = 0$) [37]. Recent papers in non-equilibrium molecular dynamic simulations of three dimensional micro-Poiseuille flows in Knudsen regime reconsider micro-channels: the influence of surface roughness, surface wetting and wall density are investigated. The results point out that the no-slip condition can be observed for Knudsen flow when the surface is rough; the surface wetting also substantially influences the velocity profiles [38]. But for smooth surfaces, as carbon nanotube walls, a slip velocity is the key for characterizing the flows. With water flowing through hydrophobic thin capillaries, there are some qualitative evidences for slippage [39]. De Gennes [40] said: *the results are unexpected and stimulating and led us to think about unusual processes which could take place near a wall*. Experimental results are connected with the thickness of the film when the thickness is of an order of the mean free path [41]. When the free mean path, denoted ℓ_{path}, is smaller than diameter $2R$ of carbon nanotubes, the Knudsen number, denoted Kn, is smaller than 1. That is the case for a liquid where the mean free path is of the same order than molecular diameters. For example in the case of liquid-water, Kn ranges between 0.5 and 10^{-2} while the nanotube radius ranges between 1 nm and 50 nm. Majunder *et al* note that *slip lengths of micron order for their experiments with nanometer size pores and the adherence boundary condition at a surface, commonly employed with the Navier-Stokes equation, is physically invalid* [19]. A slip regime occurs and the boundary condition must be changed to take account of the slippage at the solid surfaces.

We consider the simple case when $\boldsymbol{a}_1 = \boldsymbol{a}_2 \equiv \boldsymbol{a}$ and $\boldsymbol{v}_1 = \boldsymbol{v}_2 \equiv \boldsymbol{v} = [0, 0, w]$, corresponding to the same velocity and acceleration of the two-fluid mixture components. In fluid/wall slippage, the condition at the solid wall is written as

$$w = L_s \frac{\partial w}{\partial r} \quad \text{at} \quad r = R, \tag{19}$$

where L_s denotes the Navier-length [36]. The Navier-length is not independent of the thickness of the flow and may be as large as a few microns for very thin films [38, 42].
For carbon nanotubes, the dynamics of liquid flows is studied in the case of non-rough nanotubes. Equations (10) yield

$$\begin{aligned} &\rho\, \boldsymbol{a} + \rho_1 \nabla [\, \mu_1(\rho_1) - \lambda_1 \Delta\rho_1 \, - \lambda_3 \Delta\rho_2 \,] \\ &+ \rho_2 \nabla [\, \mu_2(\rho_2) - \lambda_3 \Delta\rho_1 \, - \lambda_2 \Delta\rho_2 \,] = \nu \Delta \boldsymbol{v}, \end{aligned} \tag{20}$$

where $\rho = \rho_1 + \rho_2$ and we define the dynamic viscosity of the fluid mixture ν as $\rho\,\nu = \rho_1\nu_1 + \rho_1\nu_2$; ν is assumed constant. Consequently, we consider the case when:
(i) the boundary conditions take account of the slip condition (19),
(ii) the liquid nanoflow thickness is small with respect to transverse dimensions of the wall and $2R \ll \ell_{path}$,
(iii) the flow is laminar corresponding to a velocity component along the wall large with respect to the normal velocity component to the wall which is negligible,
(iv) the permanent velocity vector $\boldsymbol{v}$ varies along the direction orthogonal to the wall, $\nabla\rho$ is normal to $\boldsymbol{v}$ and the equation of continuity reads

$$\rho \ \mathrm{div}\, \boldsymbol{v} = 0.$$

Then, the density is constant along each stream line and the trajectories are drawn on iso-density surfaces where $w = w(r)$. Due to the geometry, for permanent motions, the acceleration is null. Equations of motion separate as follows

- Along the z-coordinate, Eq. (20) yields

$$\frac{\partial p}{\partial z} = \nu \Delta w \quad \text{with} \quad \Delta w = \frac{1}{r}\frac{d}{dr}\left(r\, \frac{dw}{dr}\right) \text{ and } p = p_1 + p_2, \tag{21}$$

where p_1 and p_2 are the partial pressures of the two components.

- In the plane orthogonal to the tube axis, Eqs. (10) yield

$$\begin{aligned} &\frac{\partial}{\partial r}\left(\mu_1(\rho_1) - \lambda_1 \Delta\rho_1 \, - \lambda_3 \Delta\rho_2\right) = 0, \\ &\frac{\partial}{\partial r}\left(\mu_2(\rho_2) - \lambda_3 \Delta\rho_1 \, - \lambda_2 \Delta\rho_2\right) = 0. \end{aligned} \tag{22}$$

It is fundamental to note that Eqs (22) yield the same equations as at equilibrium. This result is the key of the distribution of densities and volume proportion between water and ethanol. Equation (21) is written as

$$\frac{1}{r}\frac{d}{dr}\left(r\, \frac{dw}{dr}\right) = -\frac{\wp}{\nu}\,, \tag{23}$$

where $\wp$ denotes the pressure gradient along the nanotube. The cylindrical symmetry of the nanotube yields the solution of Eq. (23) in the form

$$w = -\frac{\wp}{\nu}\,\frac{r^2}{4} + b,$$

where b is constant. Condition (19) implies

$$-\frac{\wp}{4\nu}R^2 + b = L_s \frac{\wp}{2\nu} R$$

and consequently,

$$w = \frac{\wp}{4\nu}\left(-r^2 + R(R + L_s)\right).$$

For liquids, the density in the nanotube is closely equal to $\rho_{\ell b} = \rho_{1\ell b} + \rho_{2\ell b}$ and the volume flow through the nanotube is

$$Q = 2\pi \int_0^R w\, r\, dr = \frac{\pi\,\wp}{8\,\nu}\, R^3(R + 4L_s).$$

Q_o denoting the Poiseuille flow corresponding to a tube of the same radius R,

$$Q = Q_o\left(1 + \frac{4L_s}{R}\right). \tag{24}$$

In most cases, the Navier length is of the micron order ($L_s = 1\,\mu m = 10^3$ nm) [19]. If we consider a nanotube with $R = 2$ nm, we obtain $Q = 2 \times 10^3\, Q_o$. For $R = 50$ nm, corresponding to the upper limit nanotube-radius for nanofluidics with respect to microfluidics, we obtain $Q = 40\, Q_o$. Consequently, the flow of liquid in nanofluidics is drastically more important than the Poiseuille flow in cylindrical tubes.
When the mixture mother-bulk is vapor, in the carbon nanotube the phase is generally liquid and the volume flow through the nanotube is approximately

$$Q = Q_o \frac{\rho_\ell}{\rho_v}\left(1 + \frac{4L_s}{R}\right).$$

In the case of water and ethanol we have $\rho_\ell/\rho_v \sim 10^2$ to 10^3 and we get a volume flow at least 10^2 time more important than the volume flow obtained by Eq. (24). Then

$$Q \sim 10^5\, Q_o\,.$$

The extremely large slip lengths measured in carbon nanotubes greatly reduce the fluid resistance and nanoscale structures could create extraordinarily fast flows as it is in biological cellular channels [43].

VII. CONCLUSIONS

In this paper, we propose a continuous model for the profile of densities between the two components of a fluid mixture. The model corresponding to the mean-field theory with hard-sphere molecules provides a free energy in the fluid mixture and an energy on the nanotube wall which yield a system of

second order differential equations for equilibrium and for dissipative motions. Depending on the wall's quality associated with the coefficients presented in Eq. (4), we obtain boundary conditions that permit to integrate the system. Thereby, carbon cylindrical nanotubes with diameters ranging from 1 to 100 nm can be studied. The carbon nanotubes are filled up with liquid mixture of water-ethanol in a volume proportion imposed by the external mixture bulk. For nanotubes of larger diameters essentially corresponding to microtubes, we obtain that the fluid phases can be liquid or vapor according to the chemical properties of the tube walls and mother bulks with possible liquid-vapor interfaces. For tubes with small diameters, essentially corresponding to nanotubes, the fluid flows are liquid mixtures and can be significantly greater than usual Poiseuille's flows, especially if the mixture mother-bulks consist of vapor.

To obtain realistic densities of liquid ethanol and liquid water, we limited to three cases of concentration ($c = 0.3, 0.5, 0.7$). The cases where c is close to 0 or 1 correspond to vapor presence of one of the constituents; thus, the composition of the mixture must be quite far from these cases. It might be interesting to take up the problem with densities for which one of the components corresponds to a vapor density but in this case, Eqs. (16) will have to be modified.

For small nanotube diameters, we notice that, in the carbon nanotube, the ratio between water and ethanol increases in favor of ethanol. These results, obtained by using a nonlinear model of continuum mechanics, are in good agreement with the simulations of molecular dynamics [44]. Recent experiments confirm these results [41, 42] and could be experimentally measured by indirect methods as Landau-squire plume measurements [36, 45].

Acknowledgements : H.G. thanks National Group of Mathematical Physics GNFM-INdAM for its support as visiting professor at the Department of Mathematics, University of Bologna.

This work was partially supported by National Group of Mathematical Physics GNFM-INdAM (A.M. and T.R.).

[1] P.J.F. Harris, Carbon nanotubes and related structures, New materials for the twenty-First century, Cambridge University Press, Cambridge, 1999.

[2] H. Gouin, *A mechanical model for the disjoining pressure*, Int. J. Eng. Sci., **47**, 691 (2009) & arXiv:0904.1809

[3] R.C. Ball and R. Evans, *The density profile of a confined fluid*, Molecular Physics, **63**, 159 (1988).

[4] J. Bear, Dynamics of fluids in porous media, Dover Publ., New York, 1988.

[5] S. Iijima, *Helical microtubules of graphitic carbon*, Nature, **354**,56 (1991).

[6] W. Krätschmer, L.D. Lamb, K. Fostiropoulos and D.R. Huffman, *Solid C_{60}: a new form of carbon*, Nature, **347**, 354 (1990).

[7] D. Mattia and Y. Gogotsi, *Review: static and dynamic behaviour of liquids inside carbon nanotubes*, Microfluid Nanofluid, **5**, 289 (2008).

[8] L. Bocquet and E Charlaix, *Nanofluidics, from bulk to interfaces*, Chem. Soc. Rev., **39**,1073 (2010).

[9] H. Gouin and W. Kosiński, *Boundary conditions for a capillary fluid in contact with a wall*, Archives of Mechanics, **50**, 907 (1998) & arXiv:0802.1995

[10] H. Gouin and T. Ruggeri, *Mixtures of fluids involving entropy gradients and accelerations waves in interfacial layers*, Eur. J. Mech./B, **24**, 596 (2005) & arXiv:0801.2096

[11] H. Gouin, A. Muracchini, T. Ruggeri, *Travelling waves near a critical point of a binary fluid mixture*, Int. J. Non-Linear Mech., **47**, 77 (2012) & arXiv:1110.5137

[12] H. Gouin, *Energy of interaction between solid surface and liquids*, J. Phys. Chem. B, **102**,1212 (1998) & arXiv:0801.4481.

[13] J. D. van der Waals, *The thermodynamic theory of capillarity under the hypothesis of continuous variation of density*, translation by J.S. Rowlinson, J. Stat. Phys., **20**, 200 (1979).

[14] J.W. Cahn and J.E. Hilliard, *Free energy of a nonuniform system. III. Nucleation in a two-component incompressible fluid*, J. Chem. Phys., **31**, 688 (1959).

[15] J.S. Rowlinson and B.Widom, Molecular theory of capillarity, Clarendon Press, Oxford, 1982.

[16] B. Widom, *What do we know that van der Waals did not know?*, Physica A, **263**, 500 (1999).

[17] H. Gouin, *Statics and dynamics of fluids in nanotubes*. Note di Matematica, **32**, 105 (2012) & arXiv:1311.2303

[18] M. Gărăjeu, H. Gouin and G. Saccomandi, *Scaling Navier-Stokes equation in nanotubes*, Phys. Fluids, **25**, 082003 (2013) & arXiv:1311.2484

[19] M. Majumder, N. Chopra, R. Andrews and B. J. Hinds, *Nanoscale hydrodynamics: Enhanced flow in carbon nanotubes*, Nature, **438**, 44 (2005).

[20] M. D. Ma, L. Shen, J. Sheridan, J. Z. Liu, C. Chen, and Q. Zheng, *Friction of water slipping in carbon nanotubes*, Phys. Rev. E, **83**, 036316 (2011).

[21] J.A. Thomas and A.J.H. McGaughey, *Reassessing fast water transport through carbon nanotubes*, Nano Lett., **8**, 2788 (2008).

[22] Y. Rocard, Thermodynamique, Masson, Paris, 1952.

[23] Ornstein, L. S. and Zernike, F., Accidental deviations of density and opalescence at the critical point of a single substance, Royal Netherlands Academy of Arts and Sciences (KNAW). Proceedings. 17, 793 (1914).

[24] F. Dell'Isola, H. Gouin and G. Rotoli, *Nucleation of spherical shell-like interfaces by second gradient theory: numerical simulations*, Eur. J. Mech., B/Fluids, **15**, 545 (1996) & arXiv:0906.1897

[25] I.E. Dzyaloshinsky, E.M. Lifshitz and L.P. Pitaevsky, *The general theory of van der Waals forces*, Adv. Phys., **10**,165 (1961).

[26] J. W. Cahn, *Critical point wetting*, J. Chem. Phys., **66**, 3667 (1977).

[27] P. G. de Gennes, *Wetting: statics and dynamics*, Rev. Mod. Phys., **57**, 827 (1985).

[28] H.C. Hamaker, *The London-van der Waals attraction between spherical particles*, Physica, **4**, 1058 (1937).

[29] J. Israelachvili, Intermolecular forces, Academic Press, New York, 1992.

[30] S. K. Mitra and S. Chakraborty, eds., Microfluidics and nanofluidics handbook: Chemistry, physics, and life science principles, CRC Press, Boca Raton, 2011.

[31] H. Gouin, *Variational theory of mixtures in continuum mechanics*, Eur. J. Mech., B/Fluids, **9**, 469 (1990) & arXiv:0807.4519

[32] B.V. Derjaguin, N.V. Chuarev and V.M. Muller, Surfaces forces,

Plenum Press, New York, 1987.
[33] R.C. Weast, Ed., Handbook of chemistry and physics, 65th ed., CRC Press, Boca Raton, 1984-1985.
[34] M. Matsumoto, A.G. Gaonkar and T. Takenaka, *The estimation of Hamaker constants of alcohols and interfacial tensions at alcohol-mercury interfaces*, Bull. Inst. Chem. Res., Kyoto Univ., **58**, 523 (1981).
[35] H. Rafii-Tabar, Computational physics of carbon nanotubes, Cambridge University Press, Cambridge, 2009.
[36] L. Landau and E. Lifchitz, Fluid mechanics, Mir Edition, Moscow, 1958.
[37] N.V. Chuarev, *Thin liquid layers*, Colloid J., **58**, 681 (1996).
[38] P. Tabeling, Introduction à la microfluidique, Librairie Belin, Paris, 2003.
[39] T.D. Blake, *Slip between a liquid and a solid - D.M. Tolstoi (1952) theory reconsidered*, Colloids Surf., **47**, 135 (1990).
[40] P. G. de Gennes, *On fluid/wall slippage*, Langmuir, **18**, 3413 (2002).
[41] E. Secchi, S. Marbach, A. Niguès, D. Stein, A. Siria and L. Bocquet, *Massive radius-dependent flow slippage in carbon nanotubes*, Nature, **537**, 210 (2016).
[42] E. Secchi, A. Niguès, L. Jubin , A. Siria and L. Bocquet, *Scaling behavior for ionic transport and its fluctuations in individual carbon nanotubes*, PRL, **116**, 154501 (2016).
[43] D.J. Bonthuis *et al*, *Theory and simulations of water flow through carbon nanotubes: prospects and pitfalls*, J. Phys. Condens. Matter, **23**, 184110 (2011).
[44] M. Mecke, J. Winkelmann and J. Fischer, *Molecular dynamics simulation of the liquid-vapour interface: The Lennard-Jones fluid*, J. Chem. Phys., **107**, 9264 (1997).
[45] E. Secchi, S. Marbach, A. Niguès, D. Stein, A. Siria and L. Bocquet, *The Landau-squire plume*, J. Fluid Mechanics, **826**, R3 (2017).